




New insight into the role of crosslinkers and composition on selectivity and kinetics of antimony uptake by chitosan-titania composite beads

Padala Abdul Nishad¹ · Anupkumar Bhaskarapillai^{1,2}  · Madapuzi P. Srinivasan¹ · Srinivasan Rangarajan¹

Received: 14 September 2020 / Accepted: 5 January 2021 / Published online: 21 January 2021

© The Author(s) 2021 

Abstract

Role of composition and the nature of crosslinking on the properties of titania-chitosan beads have been investigated in detail. The investigations were done in order to explore the feasibility of design and synthesis of titania-chitosan beads with bespoke functionality based on the intended application. This would greatly enhance the potential for the industrial application of these biopolymer based beads. Beads of varying compositions (of titania and chitosan) were prepared and crosslinked using epichlorohydrin or glutaraldehyde. The physical characteristics and antimony binding properties of the resultant crosslinked titania-chitosan beads were investigated in detail. Influence of chitosan amount on swelling was seen to be more predominant in the glutaraldehyde crosslinked beads (TA-Cts-Glu). TA-Cts-Glu beads showed more swelling and better antimony (Sb(III) and Sb(V)) uptake as compared to the epichlorohydrin crosslinked beads (TA-CTS-Epi). While TA-Cts-Glu beads showed faster uptake kinetics compared to the TA-CTS-Epi beads, the latter showed selectivity towards Sb(III) against transition metal cations. Further, the beads exhibited differential uptake of Sb(V) and Sb(III). TA-Cts-Glu beads prepared with equal amounts of titania and chitosan showed the maximum Sb(V) uptake while the TA-Cts-Epi beads with higher chitosan to titania ratio showed the least. Sb(V) binding was enhanced by the crosslinked chitosan, while the Sb(III) uptake was aided predominantly by the titania content in the beads.

Keywords Antimony · Chitosan · Selectivity · Titania · Nuclear · Crosslinker effect

1 Introduction

Removal of low-level radioactive antimony during coolant system decontamination is a difficult problem faced by most of the nuclear power plants around the world [1, 2]. Moreover, antimony is considered as an emerging drinking water pollutant and major source of antimony pollution comes from antimony mining and smelting industries [3]. USEPA has classified antimony as a pollutant of priority importance and prescribed 6 ppb as the maximum contaminant level. The WHO set guideline value for antimony in drinking water is 20 ppb. Thus, there is an increasing focus on the treatment of industrial effluents containing

antimony and research on various materials with antimony binding properties are emerging. The extent of work, however, is limited and not as wide as is seen on development of materials for the removal of regular heavy metal pollutants.

Biopolymer chitosan, in neat or modified form, has been extensively reported for various applications such as heavy metal remediation, drug delivery and biomaterials [4–9]. Crosslinking of chitosan using suitable crosslinking agents to improve its stability and reduce the solubility under acidic conditions to make them useable for sorption applications under wider solution conditions were reported [10–12]. Apart from solubility modification and

Supplementary information The online version of this article (<https://doi.org/10.1007/s42452-021-04158-7>).

✉ Anupkumar Bhaskarapillai, anup@igcar.gov.in | ¹Water and Steam Chemistry Division, Bhabha Atomic Research Centre, BARC Facilities, Kalpakkam, Tamil Nadu 603102, India. ²Homi Bhabha National Institute, Anushakthi Nagar, Mumbai, Maharashtra 400094, India.

SN Applied Sciences (2021) 3:166 | <https://doi.org/10.1007/s42452-021-04158-7>

enhanced matrix stability, crosslinking agents have wider influence on the binding properties of the chitosan [13, 14]. Nature and the degree of crosslinking in the chitosan significantly affect its sorption properties. Crosslinking involving the functional groups responsible for metal ion binding leads to reduced metal ion uptake capacity while the participation of the crosslinker moieties in metal ion binding enhances the uptake capacity. Further, crosslinking generally leads to slower sorption kinetics because of the restricted access to the binding sites.

Modification of chitosan has gained major attention in the purview of some special applications such as drinking water treatments. Chitosan has been made into composite format with different inorganic oxides such as TiO_2 and Fe_2O_3 , to make it suitable for the specialised applications [15, 16]. Through such modifications, and careful choice of crosslinkers, the sorption equilibrium and binding site selectivity of the chitosan based sorbents can be fine-tuned. This will eventually lead to the development of cheap and easy to prepare sorbent materials for the removal of various pollutants. We have earlier reported the synthesis of stable nano titania impregnated epichlorohydrin crosslinked chitosan composite beads in a format suitable for large scale applications [16]. The utility of the beads for nuclear industry have also been demonstrated through batch and column sorption experiments [2, 17].

In the current study, we have prepared crosslinked titania-chitosan beads of varying compositions using two of the most commonly used crosslinkers for chitosan namely, glutaraldehyde and epichlorohydrin. Glutaraldehyde is known to crosslink chitosan by binding with the amino functional groups of the chitosan, while epichlorohydrin is known to crosslink through the hydroxyl groups [18]. Thus, the nature of the binding sites and hence the binding properties of the crosslinked TA-Cts beads obtained are expected to be reflective of the crosslinker used. Further, the ratio of titania to chitosan used in the preparation of the beads can also affect the binding properties. To ascertain this hypothesis, we have studied in detail, the kinetic behaviour and selectivity of the beads prepared with varying compositions. The results could help in formulating the composition of the beads according to the intended application and thus enhance the potential for the use of these beads for industrial applications.

2 Experimental details

2.1 Materials and methods

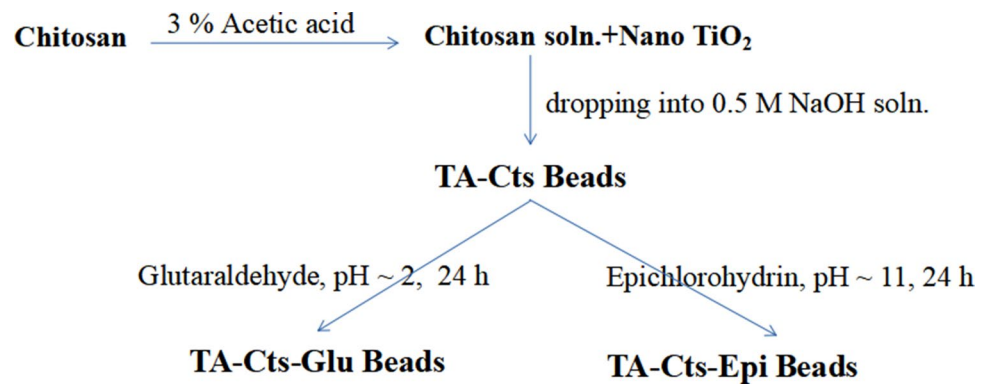
Chitosan (medium molecular weight; Catalog number 448877, molar mass (viscometry) 140,469 g/mol [19], and potassium hexahydroxoantimonate were obtained from

Sigma–Aldrich. The degree of de-acetylation (DDA in chitosan was found to be 74%. DDA was estimated by dissolving chitosan by the addition of few drops of HCl solution (1 M and back titrating the excess HCl with NaOH solution (0.1 M using pH meter [20]. Nano-titania (special grade; particle size: 10–15 nm was obtained from Travancore Titanium Products Limited, Trivandrum, India. The titania used was of anatase phase with specific surface area of 146.1 m^2/g , and 17–18% moisture content. Epichlorohydrin (minimum assay: 98.5%) and $\text{Co}(\text{NO}_3)_2 \cdot 6\text{H}_2\text{O}$ (minimum assay: 97.0%) were purchased from Loba Chemie, India. Glutaraldehyde solution (25% (W/W) solution in water), and potassium antimony(III) tartrate (LR, minimum assay: 98.5%) were obtained from SDFCL, India. $\text{Ni}(\text{NO}_3)_2 \cdot 6\text{H}_2\text{O}$ (minimum assay: 98.0%), $\text{CuSO}_4 \cdot 5\text{H}_2\text{O}$ (minimum assay: 99.0%), and $\text{K}_2\text{Cr}_2\text{O}_7$ (minimum assay: 99.9%) were obtained respectively from CDH, Qualigens, and Merck, India. All chemicals were used as supplied without further purification. Sample solutions were prepared using ultrapure water (Milli Q, Merck Millipore). Antimony and metal ion concentrations were estimated using Inductively Coupled Plasma–Atomic Emission Spectrometer (ULTIMA2 Horiba Jovin Yvon, France). A glass electrode was used for pH measurements with sensitivity of ± 0.1 . Bead sizes were estimated by processing the optical images of the beads (captured with Nikon SM2 1000 stereomicroscope) using an image processing software [21].

2.2 Preparation of the crosslinked titania-chitosan beads

The preparation of the crosslinked beads involved two steps—preparation of the non-crosslinked nano titania impregnated-chitosan (TA-Cts) beads [16] of varying titania to chitosan ratio (1:1 and 1:5, w/w), and crosslinking of these beads with epichlorohydrin or glutaraldehyde as the crosslinker. Nano-titania was dispersed in chitosan solution (in 3% acetic acid), with different TiO_2 to chitosan ratios, and then precipitated in bead format by dropping it (through 20-gauge needle attached to a syringe) into 0.5 M NaOH solution (Scheme 1) to obtain the TA-Cts beads. The TA-Cts beads thus obtained were washed several times with ultra-pure water and then subjected to crosslinking by immersing them in the respective crosslinker solutions for 24 h. The pH of the crosslinker solutions was kept between 10 and 11 (with NaOH) for crosslinking with epichlorohydrin, and between 2 and 3 (with H_2SO_4) for crosslinking with glutaraldehyde. (Scheme 1).

The crosslinked beads were then washed extensively with ultra-pure water and dried. The beads thus obtained were used for the sorption studies. The amount of various constituents used in the synthesis of the beads and the amount of final product obtained are given in Table 1.

Scheme 1. Preparation of the crosslinked titania-chitosan beads

Epichlorohydrin and glutaraldehyde crosslinked chitosan beads (Cts-Epi and Cts-Glu respectively) were also prepared in a similar fashion without the addition of nano TiO₂ (Table 1).

2.3 Swelling studies

Equilibrium Swelling Ratio (ESR), Equilibrium Water Content (EWC) and true wet density of the beads were obtained by equilibrating about 0.1 g of the beads with 14 mL of ultra-pure water (as swelling agent) in a plastic vial kept on a test tube rotator. The swelling parameters were calculated using reported procedures [17].

2.4 Sorption and desorption studies

Batch sorption studies were carried out by equilibrating a known amount of the beads in polypropylene vials containing known volumes of the antimony solutions on a rotator. Sb(V) and Sb(III) solutions were made using K₂Sb(OH)₆ and potassium antimony(III) tartrate respectively. Uptake capacities of the beads were obtained as q_e (mg g⁻¹) (Eq. 1).

$$q_e = \frac{(c_i - c_e)V}{w} \quad (1)$$

where C_i and C_e are respectively the initial and final antimony concentrations (mg L⁻¹) of the equilibrated solutions, v the volume (L) of the solution used and w , the weight (g) of the sorbent used.

Distribution constant (K_d) (L Kg⁻¹) was calculated as the ratio of concentration of the metal ion in the sorbent to the metal ion concentration of the solution at equilibrium (Eq. 2).

$$K_d^{Sb} = \frac{[Sb]_{Sorbent}}{[Sb]_{Solution}} \quad (2)$$

Sorption experiments were carried out by equilibrating 20 mg beads with 10 mL of the antimony solutions for 3 days. Desorption was carried out by treating the antimony loaded beads with 5 ml of 5 M HCl or 10 mL of 0.1 M NaOH solutions after washing them with ultrapure water. The water washings were also subjected to antimony estimations.

To find the saturation capacities of the beads, 10 mg of the respective beads were equilibrated with 2 mL of Sb(V) solutions having different initial concentrations for 5 days. Selectivity studies were carried out by equilibrating 10 mg

Table 1 Synthesis of the beads with varying composition

Legend for the sorbent beads	Constituents used in the preparation of the beads					Amount of the final product obtained (mg)
	TiO ₂ (mg)	Chitosan (mg)	Acetic acid (3% soln.) (mL)	Epichlorohydrin (mL)	Glutaraldehyde (25% soln.) (mL)	
Cts-Epi	–	335	12	0.6	–	324
1TA-5Cts-Epi	105	515	20	1	–	651
3TA-3Cts-Epi	303	307	12	0.6	–	559
Cts-Glu	–	339	12	–	2.89	424
1TA-5Cts-Glu	102	515	20	–	4.82	606
3TA-3Cts-Glu	304	306	12	–	2.89	605

of the beads with 2 mL of the solution containing 1 mM each of antimony and other ions.

2.5 Sorption kinetics

To study the sorption kinetics, 50 mg beads were equilibrated with 10 mL of the 1 mM Sb(V) solutions in batch mode. Sb(V) solutions of concentrations 0.84 mM (for 1TA-5Cts-Epi and 1TA-5Cts-Glu) and 1.06 mM (for 3TA-3Cts-Epi and 3TA-3Cts-Glu) were used for the studies. Samples were collected periodically and analysed for antimony concentrations to compute the antimony removal with equilibration time for a period of 250 h. The experimental kinetic data were fitted with the linearized forms of pseudo first order (P_1) (Eq. 3), pseudo second order (P_2) (Eq. 4) and the Weber–Morris intra-particle diffusion (IPD) models (Eq. 5).

$$\log(q_e - q_t) = \log(q_e) - \frac{k_1 t}{2.303} \tag{3}$$

Rate constant (K_1) is determined from the linear plots of $\log(q_e - q_t)$ vs. t [22].

$$\frac{t}{q_t} = \frac{1}{k_2 q_e^2} + \frac{1}{q_e} t \tag{4}$$

The sorption process governed by pseudo-second-order (P_2) model should yield a straight line with $\frac{1}{q_e}$ as the slope and $\frac{1}{k_2 q_e^2}$ as the intercept on plotting $\frac{t}{q_t}$ vs t [22].

$$q_t = K_i t^{0.5} + B_i \tag{5}$$

The plot of q_e vs $t^{0.5}$ should be linear for the sorptions which follow the Weber–Morris IPD model.

where q_t and q_e are the antimony uptake capacities of the TA-Cts beads respectively at time, ' t ' and at equilibrium. K_1 (h^{-1}), K_2 ($g\ mg^{-1}\ h^{-1}$) and K_i ($mg\ g^{-1}\ h^{-0.5}$) are the rate constants of pseudo first order, pseudo second order and intra-particle diffusion model equations respectively. Constant B_i is the initial adsorption ($mg.g^{-1}$) [23].

2.6 Equilibrium modelling of sorption isotherms

The results obtained from the equilibrium sorption studies were analysed using Langmuir, Freundlich and Dubinin–Radushkevich (D–R) isotherm models. The corresponding model constants and coefficients were determined through linear regression. The linearised form of the Langmuir isotherm is given as [22].

$$\frac{c_e}{q_e} = \frac{1}{q_{max} b} + \frac{1}{q_{max}} C_e \tag{6}$$

where q_e is the amount of Sb(V) sorbed (mmol/g) over the TA-Cts beads and c_e is the equilibrium concentration of

the Sb(V) in the solution (mmol/L). Langmuir parameters q_{max} (the monolayer adsorption capacity, mmol/g) and b , a coefficient related to the affinity between the solute and the sorbent, are obtained from the linear plots of c_e/q_e against c_e .

Linearised form of the Freundlich isotherm model is given as [22].

$$\log q_e = \log K_F + \frac{1}{n} \log C_e \tag{7}$$

The linear fit of the plot $\log q_e$ against $\log c_e$ gives the Freundlich parameters K_F (L/g) and n . An ' n ' value between 0 and 10 indicates a favourable sorption [24].

Linearised form of the Dubinin–Radushkevich (D–R) isotherm model is expressed as [22],

$$\ln q_e = \ln q_m - \beta \epsilon^2 \tag{8}$$

where q_m is the theoretical saturation capacity (mmol/g) and β ($mol^2\ J^2$) is the activity coefficient related to sorption mean free energy, E ($E = 1/\sqrt{2\beta}$). If the value of E lies between 8 and 16 kJ/mol, the sorption process is expected to involve chemical interactions and for $E < 8$ kJ/mol, the sorption process is expected to involve physical interactions [24]. ϵ is the Polanyi potential, given as.

$$\epsilon = RT \ln \left(1 + \frac{1}{C_e} \right) \tag{9}$$

where T is the absolute temperature (K), and R is the ideal gas constant ($8.314\ J\ mol^{-1}\ K^{-1}$). The linear fit of the plot of $\ln q_e$ against ϵ^2 will give the slope β , and the intercept $\ln q_m$.

3 Results and discussions

3.1 Preparation of the crosslinked titania-chitosan beads

Various methods have been reported in the literature for the preparation of chitosan based materials in bead format [25]. A general procedure for the preparation of the nano TiO₂ impregnated epichlorohydrin crosslinked chitosan composite beads was given in an earlier report [16], wherein crosslinking was carried out by adding epichlorohydrin to the titania-chitosan dispersion and then dropping the dispersion into alkaline (NaOH) solution. Thus, it involved in-situ TA-Cts bead formation and subsequent base catalysed crosslinking of chitosan in the alkaline bath. Such one pot procedure is not feasible when glutaraldehyde is used as the crosslinker as the crosslinking is to be done in acidic medium, which would lead to instant solidification of the titania-chitosan dispersion. This

would make the bead formation impossible. Hence, in this study, a modified two step procedure was followed for the preparation of both epichlorohydrin and glutaraldehyde crosslinked beads. In the first step, titania-chitosan (TA-Cts) beads with two different ratios—1:5 and 1:1—of titania and chitosan were prepared. The prepared TA-Cts beads were removed from the alkaline bath and washed extensively with ultra-pure water. In the second step, the TA-Cts beads thus obtained were crosslinked by suspending the beads in the respective crosslinker solution (containing about 25 mmol crosslinker per gram of chitosan used in the preparation of the TA-Cts beads) for 24 h. Free pendant $-NH_2$ groups present in the chitosan backbone react with glutaraldehyde to form imine groups which are stabilised through resonance with the adjacent ethylenic bonds [26]. Crosslinking may involve two chitosan monomeric units belonging either to the same polymeric chain or to two different polymeric chains. Webster et.al, have proposed a double-stranded helical coil model for the crosslinked chitosan in which an aldehyde linker from the glutaraldehyde is sandwiched between two chitosan units [12].

Epichlorohydrin can crosslink chitosan through the amino and the hydroxyl functional groups of the chitosan [27, 28], but is known to crosslink the chitosan preferably through the hydroxyl functional groups under basic conditions [29].

Crosslinking that utilises the functional groups responsible for metal ion binding normally results in the reduction in metal uptake capacity even though it imparts

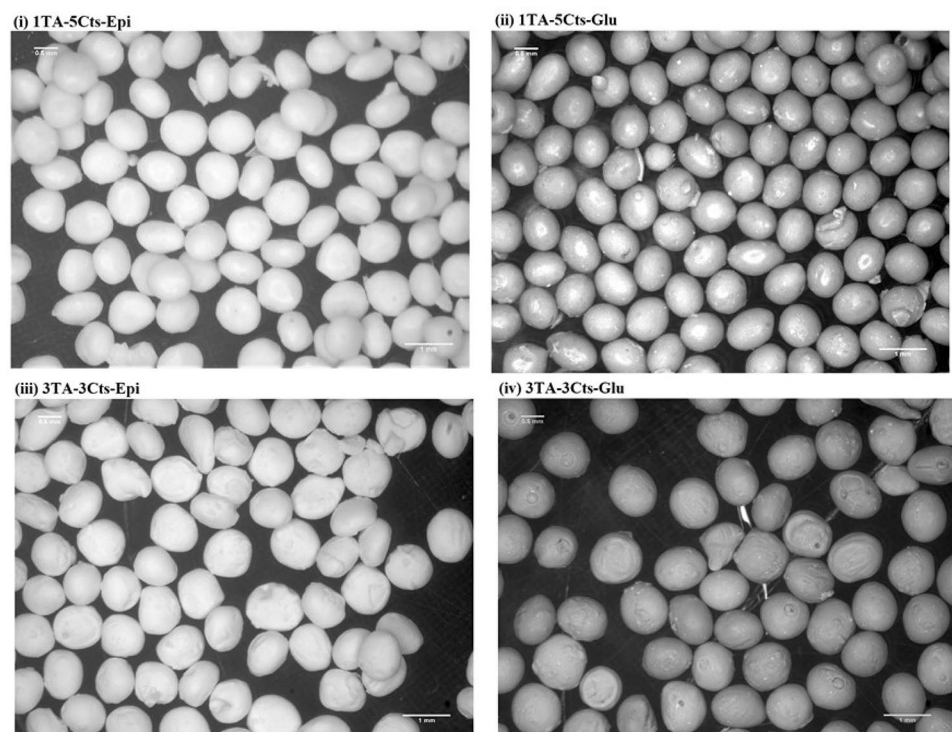
better physical and mechanical properties [10, 30]. Thus, the nature of the functional group available for binding, and hence the sorption characteristics, can be controlled by the choice of the crosslinker. For example, crosslinking through hydroxyl groups can impart selectivity for amino binding metal ions [10].

3.2 Characterisation of the beads: bead size and swelling characteristics

The optical microscope images of the beads were recorded (Fig. 1). The size distribution plots of the beads are given in Fig. 2. Beads with higher chitosan content and crosslinked with glutaraldehyde (1TA-5Cts-Glu) showed the most narrow size distribution. The optical microscope images showed the beads to be well formed with uniform shape when the chitosan content was higher than titania. This shows the role of chitosan in forming a stable matrix for the formation of composite beads.

Presence of free hydrophilic functional groups (eg. $-OH$ and $-NH_2$ groups in chitosan) and higher amorphous content in the polymer increases the swelling. Extent of swelling depends upon the polymer-solvent system and the crosslinking density. The absorption of water by non-crosslinked chitosan occurs as a result of molecular level hydration originating from its free, non-bonded hydroxyl and amino functional groups of the glucosamine moiety. In the case of crosslinked polymers, the swelling is influenced by the nature of crosslinking as well [31].

Fig. 1 Stereomicroscope images of the crosslinked titania chitosan beads of various compositions



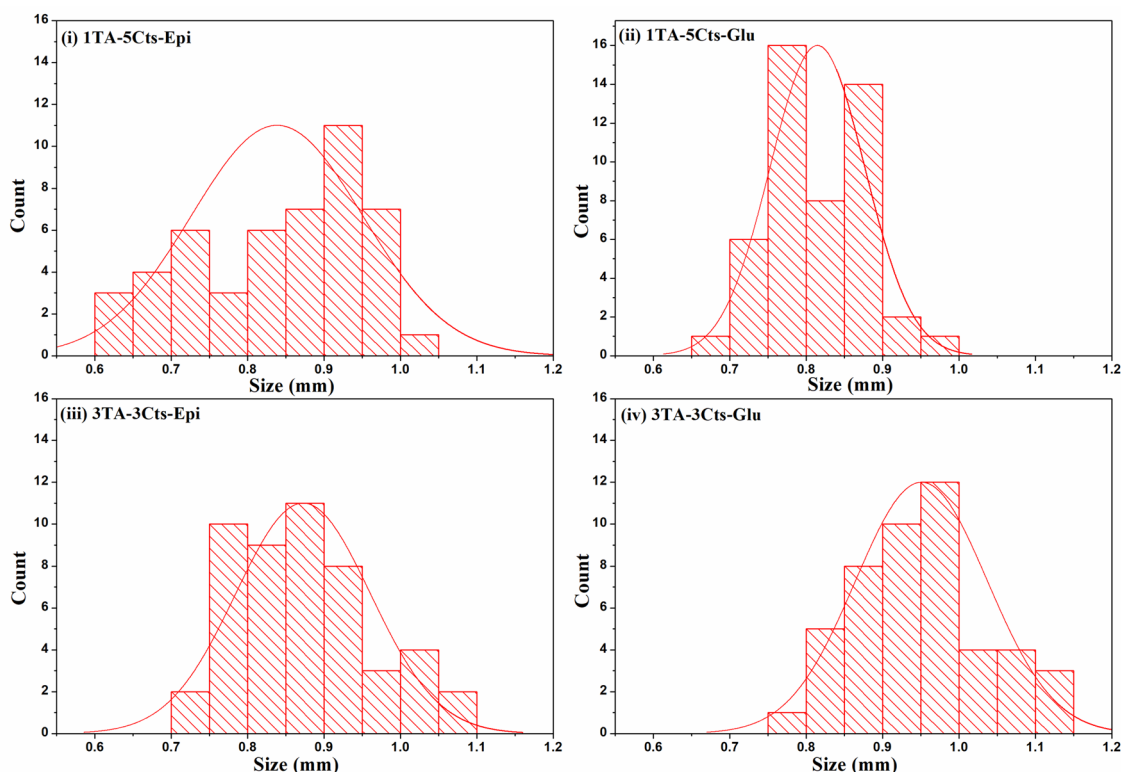


Fig. 2 Size distribution plots for the crosslinked titania chitosan beads of various compositions

Table 2 Swelling parameters of the prepared sorbent beads

Legend	Swelling characteristics			
	pH _{Eq}	ESR (%)	EWC (%)	True Wet Density (kg L ⁻¹)
Cts-Epi	3.7	54 ± 1	35 ± 1	1.260 ± 0.002
1TA-5Cts-Epi	3.9	35 ± 3	26 ± 2	1.347 ± 0.017
3TA-3Cts-Epi	5.8	35 ± 5	26 ± 3	1.498 ± 0.065
Cts-Glu	4.3	72 ± 4	42 ± 1	1.180 ± 0.004
1TA-5Cts-Glu	4.5	118 ± 1	54 ± 1	1.182 ± 0.016
3TA-3Cts-Glu	5.2	53 ± 1	35 ± 1	1.349 ± 0.033

ESR Equilibrium Swelling ratio, EWC Equilibrium Water Content

Swelling characteristics of the beads were analysed using ultra-pure water as the swelling agent. Glutaraldehyde crosslinked TA-Cts beads showed more swelling compared to the epichlorohydrin crosslinked beads (Table 2). More chitosan content in the beads was seen to render more swelling. This is more pronounced in the case of glutaraldehyde crosslinked TA-Cts beads, which is anticipated as the crosslinking was carried out on preformed beads under acidic conditions. The high yield (Table 1) and less swelling (Table 2) of the Cts-Glu beads as compared to 1TA-5Cts-Glu beads implies higher degree of crosslinking in the former than the latter.

Titania was reported to interact with the amine functional groups (through which glutaraldehyde crosslinks) of chitosan and thus lead to reduced crosslinking density [32]. Epichlorohydrin crosslinked TA-Cts beads showed comparatively higher apparent density which was seen to increase with increase in titania content in the TA-Cts beads. The enhanced swelling will have significant influence on metal uptake capacities and kinetics of the respective beads.

3.3 Sorption characteristics of the beads

3.3.1 Antimony removal by the beads: sorption and desorption

Antimony uptake properties of all the beads prepared and nano titania were investigated through batch sorption studies with Sb(V) and Sb(III) solutions. The sorbed antimony was extracted from the beads using 5 M HCl or 0.1 M NaOH. Results of the sorption and desorption studies are given in Table 3 for Sb(V) and Sb(III).

The higher antimony uptake by Cts-Epi beads compared to Cts-Glu can be attributed to the crosslinker induced uptake of antimony. It was reported that epichlorohydrin as a crosslinker could enhance the antimony uptake properties of chitosan [2, 3, 17]. Glutaraldehyde

Table 3 Antimony removal by the sorbents: sorption and desorption studies

Sb(V) (initial concentration: 0.87 mM)					
Legend	Sb(V) sorption			Antimony desorbed (%)	
	pH _{Eq}	Capacity (mg g ⁻¹)	Uptake (%)	5 M HCl	0.1 M NaOH
Cts-Epi	4.3	48.3 ± 0.8	87.4 ± 1.1	90.7	51.3
1TA-5Cts-Epi	4.1	14.6 ± 0.9	28.9 ± 1.8	61.9	13.0
3TA-3Cts-Epi	6.3	11.4 ± 0.9	20.6 ± 1.5	57.2	17.3
Cts-Glu	5.7	19.1 ± 0.5	34.0 ± 1.0	84.7	82.9
1TA-5Cts-Glu	5.7	20.8 ± 0.6	39.8 ± 1.2	96.2	78.2
3TA-3Cts-Glu	5.7	24.1 ± 0.4	44.4 ± 1.1	70.8	39.4
Nano TiO ₂	2.8	51.9 ± 0.8	95.3 ± 1.5	68.3	45.0
Sb(III) (initial concentration: 0.81 mM)					
Legend	Sb(III) sorption			Antimony desorbed (%)	
	pH _{Eq}	Capacity (mg g ⁻¹)	Uptake (%)	5 M HCl	0.1 M NaOH
Cts-Epi	4.0	37.3 ± 1.7	83.8 ± 0.6	94.9	80.8
1TA-5Cts-Epi	3.5	4.3 ± 0.7	8.8 ± 1.5	83.9	61.0
3TA-3Cts-Epi	5.1	29.0 ± 0.7	57.1 ± 2.8	94.4	22.8
Cts-Glu	5.3	32.1 ± 0.5	72.7 ± 1.3	97.6	99.9
1TA-5Cts-Glu	5.5	38.6 ± 0.5	79.7 ± 0.4	87.7	66.8
3TA-3Cts-Glu	5.8	48.2 ± 0.3	94.6 ± 0.3	93.9	29.7
Nano TiO ₂	2.7	43.8 ± 1.9	99.1 ± 1.2	93.8	39.2

crosslinked titania-chitosan (TA-Cts-Glu) beads showed better antimony (Sb(III) and Sb(V)) uptake compared to the corresponding epichlorohydrin crosslinked titania-chitosan (TA-Cts-Epi) beads. Nano TiO₂ showed the highest uptake of antimony among all the sorbents tested. Antimony uptake of the epichlorohydrin crosslinked TA-Cts beads decreased with increase in titania content. While in glutaraldehyde crosslinked TA-Cts beads, the uptake was found to increase with increase in TiO₂ content. 5 M HCl was seen to be a better eluent than 0.1 M NaOH for the desorption of antimony. Simple change in the solution pH did not bring out the bound antimony from the beads. This indicates that the antimony sorption involved stronger binding by the binding sites in the beads.

While comparing the beads prepared with same titania to chitosan ratio but with different crosslinkers (eg., 1TA-5Cts-Epi and 1TA-5Cts-Glu); antimony uptake was found to depend on the respective swelling characteristics of the beads (Fig. 3). Uptake of both Sb(V) and Sb(III) were seen to increase with increase in swelling. Higher swelling enables better accessibility to the binding sites leading to enhanced metal ion uptake.

Whereas, similar dependence of uptake on the swelling parameter was not seen among the beads prepared with the same crosslinker but with different titania to chitosan ratio. In the case of 1TA-5Cts-Glu and 3TA-3Cts-Glu beads with reducing ESR, both Sb(V) and Sb(III) uptake

were found to increase with increase in the TiO₂ content in the beads. This indicates that the TiO₂ component in the glutaraldehyde crosslinked beads plays the major role in the antimony binding.

In the case of 1TA-5Cts-Epi and 3TA-3Cts-Epi beads, though both have comparable ESR values, Sb(V) uptake was found to be more in the former, which has lower titania content (and more crosslinked chitosan) than the latter. But in the case of Sb(III), the uptake was found to increase with increase in the titania content. Thus Sb(V) pick up was enhanced by the crosslinked chitosan, while the Sb(III) uptake was aided more by the titania content in the beads.

3.3.2 Antimony removal by the crosslinked titania-chitosan beads: kinetics of Sb(V) sorption

Sorption kinetics is an important parameter which determines the column (flow-through systems) performance of the sorbents. Kinetics of antimony uptake over the beads were studied in batch mode by equilibrating 50 mg beads with 10 mL of Sb(V) (about 1 mM) solutions. The results obtained are plotted in Fig. 4(i). Glutaraldehyde crosslinked titania-chitosan beads showed faster uptake kinetics compared to the epichlorohydrin crosslinked beads. This implies that the former could be a better choice for use under flow conditions (column mode).

Fig. 3 Influence of equilibrium swelling ratio and the bead composition on antimony uptake (as percentage removal) by the crosslinked titania-chitosan beads

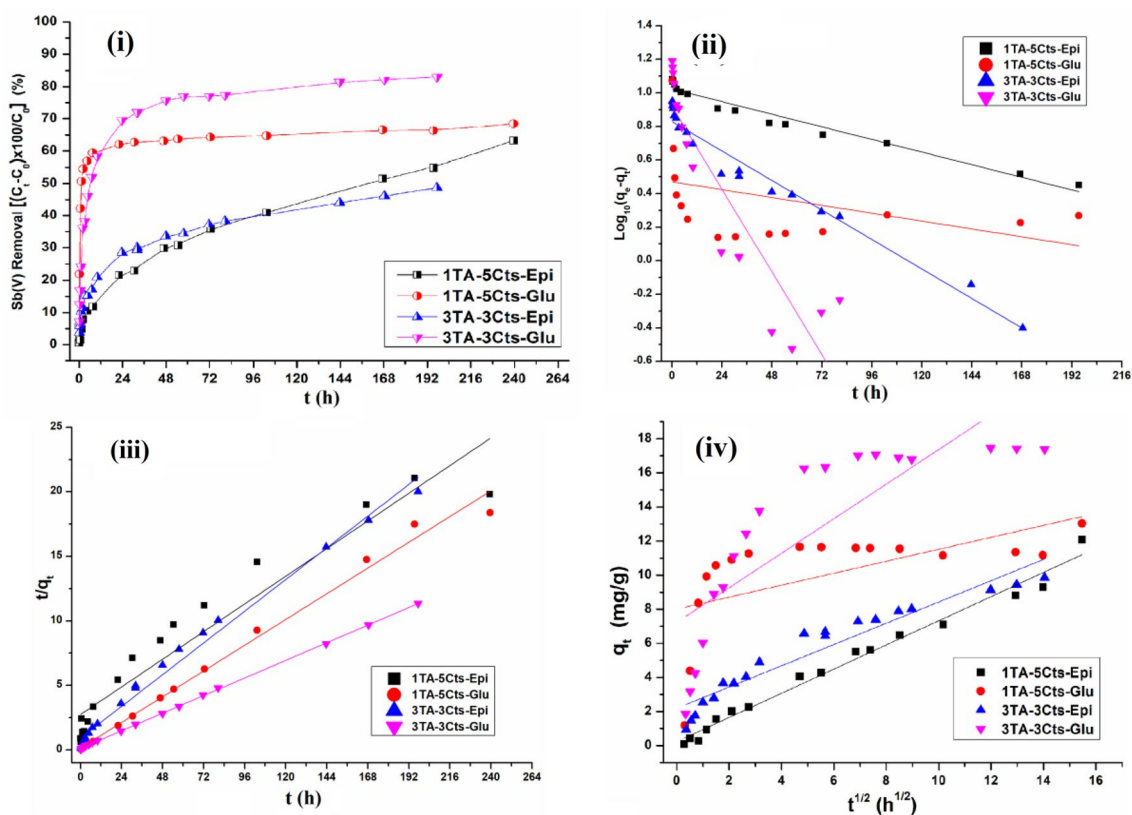
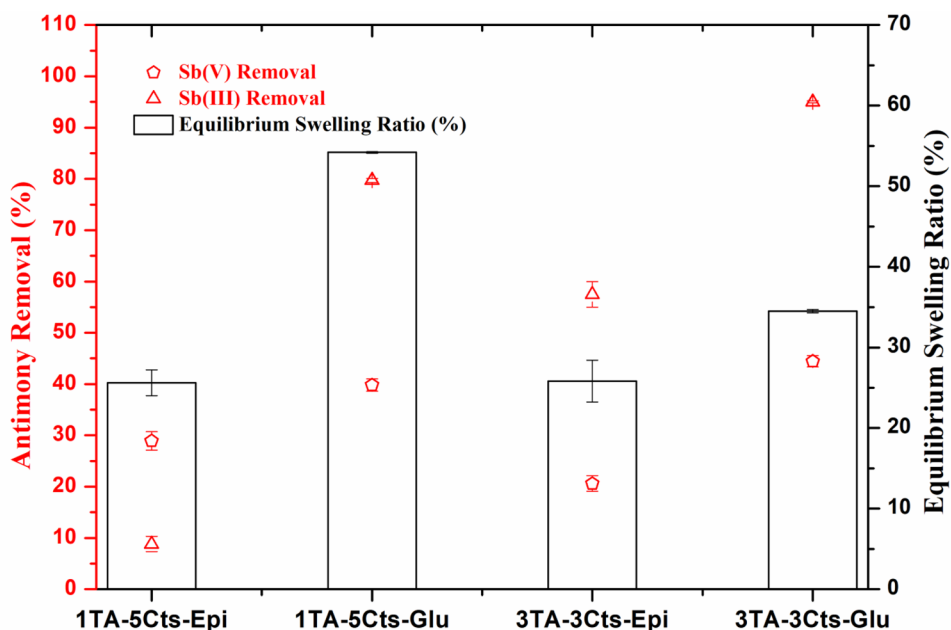


Fig. 4 Kinetics of Sb(V) uptake by the crosslinked titania-chitosan beads: (i) Change in uptake with equilibration time; (ii) Pseudo first order (iii) Pseudo second order and (iv) Intra-particle diffusion model plots for the Sb(V) sorption

3.3.2.1 Modelling of the Sb(V) sorption kinetics Sorption kinetics depends on the sorbate–sorbent interactions and operating conditions. Modelling of the kinetic behaviour

is helpful in predicting the uptake rates and also for giving insights into the sorption mechanisms. A number of mathematical models have been proposed for describ-

ing the sorption kinetics data, which may generally be classified into two categories as surface reaction models (i.e., adsorption kinetics governed by the rate of surface reactions) and diffusion models (i.e., adsorption kinetics governed by the rate of diffusion) [33]. The experimentally obtained kinetic data were fit into the linearised forms of three kinetic models namely, the Lagergren’s pseudo first order rate equation (P_1), the pseudo second order rate equation (P_2), and the Weber–Morris intra-particle diffusion (IPD) model. As per Lagergren’s pseudo first-order rate equation, the rate of sorption depends on the sorption capacity of the sorbent. The corresponding rate constant (K_1) values obtained from the sorption studies is given Table 4. Epichlorohydrin crosslinked TA-Cts beads (1TA-5Cts-Epi and 3TA-3Cts-Epi) were found to follow the pseudo-first order rate equation (Fig. 4(ii)).

Kinetics of Sb(V) sorption on TA-Cts beads was found to follow the P_2 model in general (Fig. 4(iii)). The P_2 rate constant, K_2 , was found to be higher for the glutaraldehyde crosslinked TA-Cts beads indicating better uptake kinetics. It is seen that the match between the model derived capacity values (q_e) and the experimentally obtained values is better with the P_2 model as compared to the P_1 model (Table 4).

Azizian [34] had proposed a method for deriving the P_1 and P_2 rate equations from a general rate equation for a system in equilibrium involving sorption and desorption, given as.

$$\frac{d\theta}{dt} = k_a(c_0 - \beta\theta)(1 - \theta) - k_d\theta \tag{10}$$

where θ is the coverage fraction ($0 \leq \theta \leq 1$), C_0 is the initial molar concentration of solute, k_a and k_d the adsorption

and desorption rate constants respectively. β is given as, at equilibrium,

$$\beta = \frac{c_0 - c_e}{\theta_e} \tag{11}$$

c_e is the equilibrium molar concentration of solute and θ_e is the equilibrium coverage fraction. It is suggested that through this method, the conditions that determine the application of either of the two models (P_1 or P_2) could be determined. It was shown that at high initial concentration of solute (sorbate) (i.e., $c_0 \gg \beta\theta$) the general rate Eq. (6) converts to a pseudo-first-order model, while at lower initial concentration of solute, $\beta\theta$ term becomes significant and it converts to a pseudo-second-order model. β dependency on the maximum uptake capacity of the sorbent is given as.

$$\beta = \frac{m_c q_m}{M_w V} \tag{12}$$

where m_c is the mass (g) of sorbent, q_m , the maximum capacity of sorbent, M_w , the molar weight of solute (g/mol), and V , the volume of solution (L). Hence, for the same c_0 values, sorbents with limited uptake capacity are expected to follow the P_1 model. This implies that epichlorohydrin crosslinked TA-Cts beads follow the P_1 rate equation because of the limited capacity and coverage fraction. So epichlorohydrin as a crosslinker may be utilising the functional groups responsible for the antimony sorption (thereby reducing the uptake capacity) or may be limiting accessibility of the binding sites (reducing the surface coverage factor) compared to glutaraldehyde. Both P_1 and P_2 models can encompass different rate controlling mechanisms and hence a specific sorption mechanism cannot be

Table 4 Kinetic parameters for the Sb(V) sorption over the crosslinked titania-chitosan beads

Kinetic Model	Parameter	1TA-5Cts-Epi	1TA-5Cts-Glu	3TA-3Cts-Epi	3TA-3Cts-Glu
Pseudo-First Order	$K_1 \times 10^3$ (h^{-1})	7.208	4.491	16.858	47.304
	q_e ($mg\ g^{-1}$)	10.554	2.955	6.756	8.292
	R^2	0.9590	0.1105	0.9634	0.8134
Pseudo-Second Order	$K_2 \times 10^3$ ($g\ mg^{-1}\ h^{-1}$)	2.906	48.778	11.298	26.025
	q_e ($mg\ g^{-1}$)	11.198	12.038	9.772	17.593
	R^2	0.9231	0.9916	0.9885	0.9998
Intra-Particle Diffusion	$K_f \times 10^2$ ($mg\ g^{-1}\ h^{-1/2}$)	70.904	35.077	62.383	101.295
	B_1 ($mg\ g^{-1}$)	0.23303	8.0092	2.1882	7.2352
	R^2	0.9830	0.2916	0.9173	0.6521

proposed based on the parameters derived through these models alone [35, 23].

To get more insights into the rate controlling steps that operate during the sorption, IPD model proposed by Weber and Morris was applied [22]. Slope of the plot, q_e vs $t^{0.5}$, gives k_i , the IPD model rate constant, and intercept gives B_i , which is proportional to the boundary layer thickness [23]. Epichlorohydrin crosslinked TA-Cts beads were found to follow the IPD model throughout the sorption (Fig. 4(iv)). Larger B_i value (Table 4) for 3TA-3Cts-Epi beads indicate large film diffusion resistance in the beads as compared to the 1TA-5Cts-Epi beads [22].

3.3.3 Antimony removal by the crosslinked titania-chitosan beads: initial Sb(V) concentration variation

In order to find out the saturation capacities of the different beads prepared, the beads were equilibrated with Sb(V) solutions of different initial concentrations. Sb(V) uptake capacities obtained for the different beads along with the percentage removal of antimony at different initial Sb(V) concentrations are shown in Fig. 5.

Glutaraldehyde crosslinked beads showed better antimony uptake compared to the epichlorohydrin crosslinked

ones. While for the same type of crosslinker, Sb(V) uptake capacity was found to increase with increase in titania content. 3TA-3Cts-Glu beads showed the maximum Sb(V) uptake (of 44.1 mg g^{-1}) (0.362 mmol/g) while 1TA-5Cts-Epi beads showed the least (10.4 mg g^{-1}) (0.085 mmol/g).

3.3.3.1 Modelling of the sorption equilibrium: isotherm plots

Isotherm models are helpful in comparison and selection of the sorbents for the targeted application. Langmuir model is one of the widely used models for the equilibrium sorption modelling. It assumes monolayer sorption over an energetically and structurally homogeneous surface with a finite number of identical binding sites. Also, a nil interaction—associative or dissociative—is assumed between the sorbed ions.

The Langmuir plots for the Sb(V) sorption over the TA-Cts beads are shown in Supplementary Material (Figure S1a). 1TA-5Cts-Epi beads were found to show the best fit for the Langmuir isotherm model and the theoretical monolayer adsorption capacities were found to match with the experimentally observed ones (Table 5).

The Sb(V) sorption data was also fitted with Freundlich adsorption isotherm model, which takes into account the heterogeneous binding sites and multilayer adsorption.

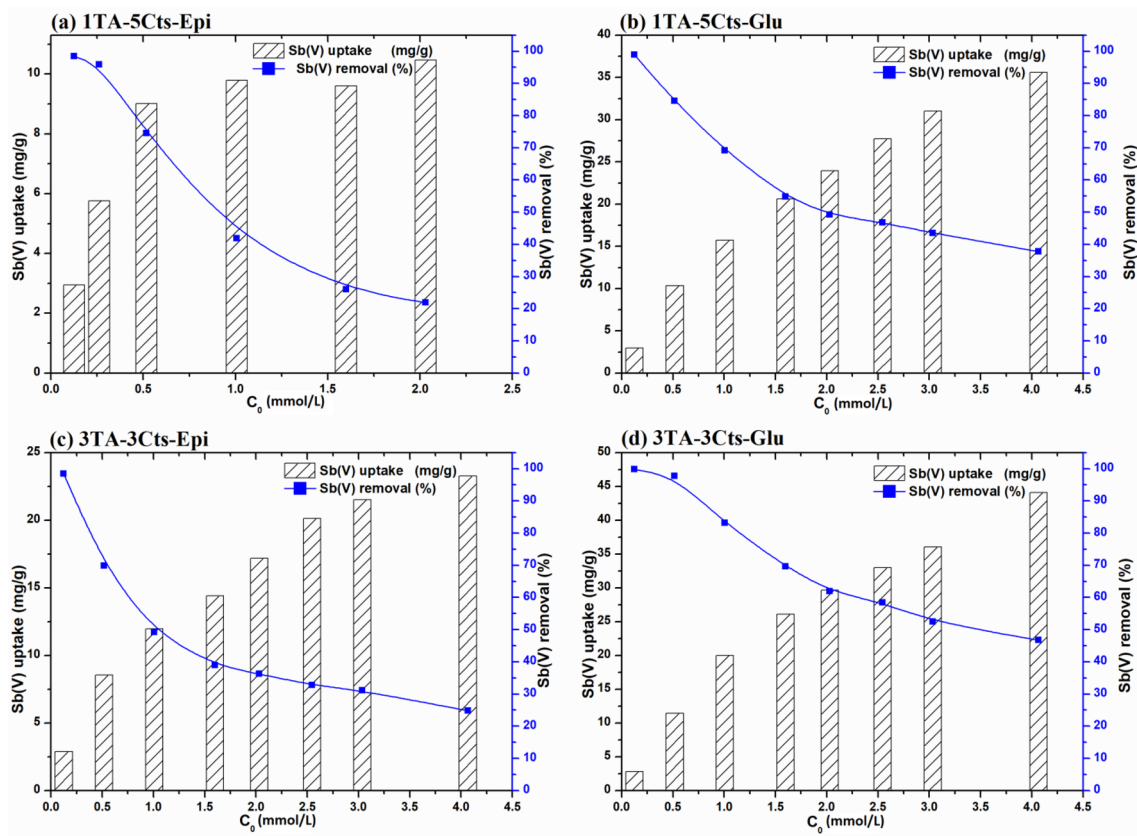


Fig. 5 Effect of initial concentration on Sb(V) uptake by the crosslinked titania-chitosan beads

Table 5 Isotherm parameters obtained for the various models for Sb(V) sorption ($T = 28 \pm 3$ °C)

Isotherm Model	Parameter	1TA-5Cts-Epi	1TA-5Cts-Glu	3TA-3Cts-Epi	3TA-3Cts-Glu
Langmuir	q_{\max} (mmol g ⁻¹)	0.0842	0.3106	0.2045	0.3546
	b	5.588×10^{-2}	2.840×10^{-3}	2.580×10^{-3}	5.420×10^{-3}
	R ²	0.9963	0.9284	0.9485	0.9495
Freundlich	K_F (L g ⁻¹)	26.35	20.97	17.98	37.99
	n	5.8408	3.0479	3.4774	3.4913
	R ²	0.8630	0.9935	0.9834	0.9884
D-R	q_m (mmo g ⁻¹)	0.1318	0.4433	0.2706	0.5090
	B (mol ² J ⁻²)	1.4672×10^{-9}	2.6825×10^{-9}	2.4068×10^{-9}	2.185×10^{-9}
	E (kJ mol ⁻¹)	18.46	13.65	14.41	15.13
	R ²	0.9187	0.9652	0.9482	0.9889

All the crosslinked beads, except 1TA-5Cts-Epi, were found to follow the Freundlich isotherm model (Fig. S1b). The 'n' values were found to fall in the 0 to 10 region (Table 5) indicating a favourable sorption [24]. Most of the TA-Cts beads showed better fit with the Freundlich isotherm than with the Langmuir isotherm indicating the heterogeneity of the binding sites in the sorbent.

To determine the nature of interactions involved in the sorption (i.e., chemical or physical interactions), sorption data were fitted with the Dubinin–Radushkevich (D–R) isotherm model. Glutaraldehyde crosslinked beads showed a comparatively better fit for the D–R isotherm equation (Fig. S1c, Table 5). The E (kJ/mol) value was found to be in 8–16 kJ/mol range for most of the TA-Cts beads implying the sorption involves chemical interactions rather than physical interactions [24].

3.3.4 Metal ion selectivity of the beads

Preferential sorption of various ions over the crosslinked titania-chitosan beads have been ascertained by equilibrating the beads with different metal ion solutions. To study the Sb(V) selectivity in presence of Cr(VI), another well-known pollutant known to exist as anionic species, sorption studies were carried out by treating the beads with 2 mL of the solution containing both Sb(V) and Cr(VI). Desorption of the sorbed ions were carried out using 2 mL of 0.1 M NaOH solution. The beads were

found to sorb Cr(VI) preferentially compared to Sb(V). Also, the beads were found to strongly bind the Cr(VI) ions compared to Sb(V), as indicated by the lower desorption of the former (Table 6). This is anticipated as the anionic Cr(VI) species is known to have strong binding affinity for most anion receptors [36].

There was no visible effect of the nature of crosslinker on the selectivity against Cr(VI) under the conditions studied.

To know the antimony selectivity of the beads against other transition metal cations, sorption studies were carried out using 10 mg of the beads with 2 mL of the solution containing 1 mM each of Sb(III) (as Sb(III)-Tartarate), Co(II), Ni(II) and Cu(II). Epichlorohydrin crosslinked TA-Cts beads showed more selectivity towards Sb(III) (Table 7).

1TA-5Cts-Glu beads showed preferential sorption of Cu(II) compared to other cations, and an increase in titania content in the TA-Cts-Glu beads (i.e., 3TA-3Cts-Glu beads) was found to increase the preferential sorption of antimony over Cu(II). This indicates that the preferential sorption of Cu(II) (by the 1TA-5Cts-Glu beads) was effected by the chitosan component. Chitosan is known for its high selectivity for Cu(II) [37]. Such preferential sorption of Cu(II) was not seen with the 1TA-5Cts-Epi beads, indicating the antimony selectivity of the epichlorohydrin crosslinked chitosan component of the beads. Further, increase in antimony uptake with increase in titania content shows the role played by TiO₂ in the

Table 6 Antimony selectivity of the crosslinked titania-chitosan beads against Cr(VI)

Sorbent	pH _{eq}	Sorption				Desorption (%)	
		Sb(V)		Cr(VI)		Sb(V)	Cr(VI)
		(%)	K _d (L kg ⁻¹)	(%)	K _d (L kg ⁻¹)		
1TA-5Cts-Epi	3.4	13 ± 3	29 ± 7	100	–	89 ± 9	4.4 ± 0.1
1TA-5Cts-Glu	6.8	53 ± 1	214 ± 2	100	–	74 ± 4	26.4 ± 0.6
3TA-3Cts-Epi	7.4	38 ± 2	116 ± 9	63 ± 1	32 ± 10	47 ± 1	15 ± 1
3TA-3Cts-Glu	6.5	78 ± 1	714 ± 8	100	–	61 ± 1	23 ± 1

Table 7 Antimony selectivity of the crosslinked titania chitosan beads against metal cations

Sorbate\Sorbent		1TA-5Cts-Epi	1TA-5Cts-Glu	3TA-3Cts-Epi	3TA-3Cts-Glu
Sb(III)	Removal (%)	15 ± 2	90 ± 1	89 ± 1	98 ± 1
	Kd (L Kg ⁻¹)	33 ± 7	1726 ± 58	1530 ± 30	8405 ± 1906
Co(II)	Removal (%)	BDL	12 ± 2	0	7 ± 2
	Kd (L Kg ⁻¹)	0	25 ± 5	0	14 ± 4
Ni(II)	Removal (%)	BDL	18 ± 1	0	4.9 ± 0.3
	Kd (L/Kg)	0	42 ± 3	0	10 ± 1
Cu(II)	Removal (%)	< 1	99 ± 1	28 ± 4	69 ± 1
	Kd (L/Kg)	< 1	23,621 ± 6739	76 ± 17	412 ± 26
pH _{eq}		3.6	5.4	5.2	4.5

BDL Below detectable level

preferential sorption of antimony by the crosslinked titania-chitosan beads.

4 Conclusion

This study, for the first time, has examined the influence of the constituents of the crosslinked titania-chitosan composite beads in detail. The dependence of the binding site properties and the physical characteristics of the composite beads on nature of the crosslinker and the ratio of chitosan to titania used in the bead preparation has been clearly brought out, including a detailed investigation of the kinetic behaviour. The composition was shown not only to influence the selectivity of the chitosan based composite beads for antimony against other metal ions, but the selectivity between the two oxidation states of antimony as well. The results have thus clearly revealed the effect of the constituents on capacity, selectivity, and kinetics. Glutaraldehyde crosslinked titania-chitosan beads showed better swelling and sorption characteristics compared to epichlorohydrin crosslinked beads. Glutaraldehyde crosslinked titania-chitosan is thus a better choice for use in the column mode of operations owing to its faster sorption kinetics. Epichlorohydrin is a better choice as a crosslinker in terms of the selectivity for antimony.

These results would help in rational design of titania-chitosan beads based on the envisaged application. Comprehensive investigations on the combined effect of antimony speciation, for example complexed as compared to free antimony species, and the polymer composition on sorption properties could yield detailed information on the binding site chemistry. Further, as antimony and arsenic share similar binding characteristics, these results would help in devising effective arsenic removal materials as well.

Compliance with ethical standards

Conflict of interest The authors have no conflicts of interest to declare that are relevant to the content of this article.

Open Access This article is licensed under a Creative Commons Attribution 4.0 International License, which permits use, sharing, adaptation, distribution and reproduction in any medium or format, as long as you give appropriate credit to the original author(s) and the source, provide a link to the Creative Commons licence, and indicate if changes were made. The images or other third party material in this article are included in the article's Creative Commons licence, unless indicated otherwise in a credit line to the material. If material is not included in the article's Creative Commons licence and your intended use is not permitted by statutory regulation or exceeds the permitted use, you will need to obtain permission directly from the copyright holder. To view a copy of this licence, visit <http://creativecommons.org/licenses/by/4.0/>.

References

1. Neeb KH (2011) The radiochemistry of nuclear power plants with light water reactors. Walter de Gruyter, Berlin
2. Nishad PA, Bhaskarapillai A, Velmurugan S (2017) Removal of antimony over nano titania-impregnated epichlorohydrin-crosslinked chitosan beads from a typical decontamination formulation. Nucl Technol 197(1):88–98
3. Nishad PA, Bhaskarapillai A, Velmurugan S (2017) Towards finding an efficient sorbent for antimony: comparative investigations on antimony removal properties of potential antimony sorbents. Int J Environ Sci Technol 14(4):777–784
4. El Knidri H, Belaabed R, Addaou A, Laajeb A, Lahsini A (2018) Extraction, chemical modification and characterization of chitin and chitosan. Int J Biol Macromol 120:1181–1189
5. Hamed I, Özogul F, Regenstein JM (2016) Industrial applications of crustacean by-products (chitin, chitosan, and chitooligosaccharides): a review. Trends Food Sci Technol 48:40–50
6. Pestov A, Bratskaya S (2016) Chitosan and its derivatives as highly efficient polymer ligands. Mol (Basel, Switzerland) 21(3):330–330
7. Rodríguez-Vázquez M, Vega-Ruiz B, Ramos-Zúñiga R, Saldaña-Koppel DA, Quiñones-Olvera LF (2015) Chitosan and Its potential use as a scaffold for tissue engineering in regenerative medicine. Biomed Res Int 2015:821279–821279

8. Shariatinia Z (2019) Pharmaceutical applications of chitosan. *Adv Coll Interface Sci* 263:131–194
9. Yong SK, Shrivastava M, Srivastava P, Kunhikrishnan A, Bolan N (2015) Environmental applications of chitosan and its derivatives. In: Whitacre DM (ed) *Reviews of environmental contamination and toxicology*, vol 233. Springer International Publishing, Cham, pp 1–43
10. Nishad PA, Bhaskarapillai A, Velmurugan S, Narasimhan SV (2012) Cobalt (II) imprinted chitosan for selective removal of cobalt during nuclear reactor decontamination. *Carbohydr Polym* 87(4):2690–2696
11. Vieira RS, Oliveira MLM, Guibal E, Rodríguez-Castellón E, Beppu MM (2011) Copper, mercury and chromium adsorption on natural and crosslinked chitosan films: an XPS investigation of mechanism. *Colloids Surf A* 374(1):108–114
12. Webster A, Halling MD, Grant DM (2007) Metal complexation of chitosan and its glutaraldehyde cross-linked derivative. *Carbohydr Res* 342(9):1189–1201
13. Sencadas V, Correia DM, Ribeiro C, Moreira S, Botelho G, Gómez Ribelles JL, Lanceros-Mendez S (2012) Physical-chemical properties of cross-linked chitosan electrospun fiber mats. *Polym Test* 31(8):1062–1069
14. Subramanian A, Lin H-Y (2005) Crosslinked chitosan: its physical properties and the effects of matrix stiffness on chondrocyte cell morphology and proliferation. *J Biomed Mater Res Part A* 75A(3):742–753
15. Ahmad R, Mirza A (2018) Facile one pot green synthesis of Chitosan-Iron oxide (CS-Fe₂O₃) nanocomposite: removal of Pb(II) and Cd(II) from synthetic and industrial wastewater. *J Clean Prod* 186:342–352
16. Nishad PA, Bhaskarapillai A, Velmurugan S (2014) Nano-titania-crosslinked chitosan composite as a superior sorbent for antimony (III) and (V). *Carbohydr Polym* 108:169–175
17. Nishad PA, Bhaskarapillai A, Velmurugan S (2017) Enhancing the antimony sorption properties of nano titania-chitosan beads using epichlorohydrin as the crosslinker. *J Hazard Mater* 334:160–167
18. Kildeeva NR, Perminov PA, Vladimirov LV, Novikov VV, Mikhailov SN (2009) About mechanism of chitosan cross-linking with glutaraldehyde. *Russ J Bioorg Chem* 35(3):360–369
19. Garcia LGS, Guedes GMDM, da Silva MLQ, Castelo-Branco DSCM, Sidrim JJC, Cordeiro RDA, Rocha MFG, Vieira RS, Brilhante RSN (2018) Effect of the molecular weight of chitosan on its antifungal activity against *Candida* spp. In planktonic cells and biofilm. *Carbohydr Polym* 195:662–669
20. Gupta KC, Jabrail FH (2006) Effects of degree of deacetylation and cross-linking on physical characteristics, swelling and release behavior of chitosan microspheres. *Carbohydr Polym* 66:43–54
21. Rasband WS, ImageJ US (1997) National Institutes of Health, Bethesda, Maryland, USA, <<https://imagej.nih.gov/ij/>, 1997–2018> (last accessed on 30/07/2020)
22. Samadi N, Hasanzadeh R, Rasad M (2015) Adsorption isotherms, kinetic, and desorption studies on removal of toxic metal ions from aqueous solutions by polymeric adsorbent. *J Appl Polym Sci* 132:11
23. Tan KL, Hameed BH (2017) Insight into the adsorption kinetics models for the removal of contaminants from aqueous solutions. *J Taiwan Inst Chem Eng* 74:25–48
24. Daneshvar E, Kousha M, Jokar M, Koutahzadeh N, Guibal E (2012) Acidic dye biosorption onto marine brown macroalgae: isotherms, kinetic and thermodynamic studies. *Chem Eng J* 204–206:225–234
25. Agnihotri SA, Mallikarjuna NN, Aminabhavi TM (2004) Recent advances on chitosan-based micro- and nanoparticles in drug delivery. *J Control Release* 100(1):5–28
26. Monteiro OAC, Airoidi C (1999) Some studies of crosslinking chitosan–glutaraldehyde interaction in a homogeneous system. *Int J Biol Macromol* 26(2):119–128
27. Li C, Cui J, Wang F, Peng W, He Y (2016) Adsorption removal of Congo red by epichlorohydrin-modified cross-linked chitosan adsorbent. *Desalination Water Treat* 57(30):14060–14066
28. Seki Y, Yurdakoc K (2008) Synthesis of pH dependent chitosan-EPI hydrogel films and their application for in vitro release of promethazine hydrochloride. *J Appl Polym Sci* 109(1):683–690
29. Chen A-H, Liu S-C, Chen C-Y, Chen C-Y (2008) Comparative adsorption of Cu(II), Zn(II), and Pb(II) ions in aqueous solution on the crosslinked chitosan with epichlorohydrin. *J Hazard Mater* 154(1):184–191
30. Wei YC, Hudson SM, Mayer JM, Kaplan DL (1992) The crosslinking of chitosan fibers. *J Polym Sci Part A Polym Chem* 30(10):2187–2193
31. Lee S-H, Park S-Y, Choi J-H (2004) Fiber formation and physical properties of chitosan fiber crosslinked by epichlorohydrin in a wet spinning system: The effect of the concentration of the crosslinking agent epichlorohydrin. *J Appl Polym Sci* 92(3):2054–2062
32. Al-Sagheer FA, Merchant S (2011) Visco-elastic properties of chitosan–titania nano-composites. *Carbohydr Polym* 85(2):356–362
33. Qiu H, Lv L, Pan B-C, Zhang Q-J, Zhang W-M, Zhang Q-X (2009) Critical review in adsorption kinetic models. *J Zhejiang Univ-Sci A* 10(5):716–724
34. Azizian S (2004) Kinetic models of sorption: a theoretical analysis. *J Colloid Interface Sci* 276(1):47–52
35. Plazinski W, Rudzinski W, Plazinska A (2009) Theoretical models of sorption kinetics including a surface reaction mechanism: a review. *Adv Coll Interface Sci* 152(1):2–13
36. Thangaraj V, Bhaskarapillai A, Velmurugan S (2020) Synthesis of a crosslinked poly(ionic liquid) and evaluation of its antimony binding properties. *J Hazard Mater* 384:121481
37. Padala AN, Bhaskarapillai A, Velmurugan S, Narasimhan SV (2011) Sorption behaviour of Co(II) and Cu(II) on chitosan in presence of nitrilotriacetic acid. *J Hazard Mater* 191(1):110–117

Publisher's Note Springer Nature remains neutral with regard to jurisdictional claims in published maps and institutional affiliations.